Computers and Electronics in Agriculture 193 (2022) 106684

Contents lists available at ScienceDirect

Computers and Electronics in Agriculture

journal homepage: www.elsevier.com/locate/compag

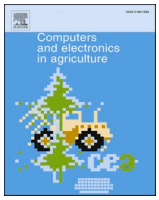

Robotic Fertilization in Strip Cropping using a CNN Vegetables Detection-Characterization Method

Christyan Cruz Ulloa [1,*], Anne Krus [2], Antonio Barrientos [1], Jaime del Cerro [1], Constantino Valero [2]

Centro de Automática y Robótica, Consejo Superior de Investigaciones Científicas, Universidad Politécnica de Madrid, 28006 Madrid, Spain
Departamento de Ingeniería Agroforestal, ETSI Agronómica, Alimentaria y de Biosistemas, Universidad Politécnica de Madrid, 28040 Madrid, Spain

ARTICLE INFO

Keywords:
Organic farming
Strip cropping
ROS
Robotic systems
Convolutional Neural Networks
Deep Learning

ABSTRACT

To meet the increased demand for organic vegetables and improve their product quality, the Sureveg CORE Organic Cofund ERA-Net project focuses on the benefits and best practices of growing different crops in alternate rows. A prototype of a robotic platform was developed to address the specific needs of this field type at an individual plant level rather than per strip or field section. This work describes a novel method to develop robotic fertilization tasks in crop rows, based on automatic vegetable Detection and Characterization (D.a.C) through an algorithm based on artificial vision and Convolutional Neural Networks (CNN). This network was trained with a data-set acquired from the project's experimental fields at ETSIAAB-UPM. The data acquisition, processing, anc actuation are carried out in Robot Operating System (ROS). The CNN's precision, recall, and IoU values as well as characterization errors were evaluated in field trials. Main results show a neural network with an accuracy of 90.5% and low error percentages (<3%) during the vegetable characterization. This method's main contribution focuses on developing an alternative system for the vegetable D.A.C for individual plant treatments using CNN and low-cost RGB sensors.

1. Introduction

The global increase in food consumption has increased the demand for more and better harvests (Gouel and Guimbard, 2019). One of the main options focuses on applying new cultivation techniques, i.e. applying robotic systems and automation processes, improving the quality of cultivated vegetables to meet this food demand (Kulkarni et al., 2020). Additionally, a focus on reducing herbicides and harmful solutions such as fertilizers mitigates the polluting effects on water, soils, and the atmosphere (Silva et al., 2020).

The advantages of using robotic systems within precision agriculture are numerous. The automation of fertilization and seeding tasks, the optimization of fertilizer dosages, and the application of liquid fertilizers to specific areas of the plant stand out, as well as specialized analysis of the vegetative state (Naik et al., 2016; Asefpour Vakilian et al., 2017; Ren et al., 2020; Zhang and Karkee, 2021; Nguyen et al., 2017; Campos et al., 2016). These tasks are developed using robotic manipulators and specific sensors to identify plants and their specific needs. Examples of employed sensors are RGB cameras(Manasa et al., 2019; Magalhães et al., 2021; Campos et al., 2017), multi-spectral (MS) cameras(Paoletti et al., 2019), and lasers. Lately, machine learning algorithms are gaining ground in processing the data these sensors produce, as e.g. in (Kulkarni et al., 2020; Liu and Wang, 2020).

Recent works that apply convolutional neural networks (CNN) within agriculture focus on recognizing pests and diseases in vegetables (Liu and Wang, 2020; Zhang et al., 2019; Sakai et al., 2016; Zeng, 2017), fruit classification (Sun et al., 2021; Steinbrener et al., 2019; Álvarez-Canchila et al., 2020), vegetable detection (Ikeda et al., 2018; Li et al., 2020; Ma et al., 2017; Kuznetsova et al., 2020), and damage in plantations(HamidiSepehr et al., 2019). Furthermore, applications are being developed that focus on yield estimation and planting using field robots (Gonzalez-de Santos et al., 2020; Oliveira et al., 2021). In robotic fertilization, the main developments focus on analyzing the entire plantation at once using classical vision. The fertilizer is subsequently

* Corresponding author at: Centro de Automática y Robótica, Consejo Superior de Investigaciones Científicas, Universidad Politécnica de Madrid, 28006 Madrid, Spain.
E-mail addresses: christyan.cruz@car.upm-csic.es, christyan.cruz.ulloa@alumnos.upm.es (C. Cruz Ulloa).
[1] CAR-UPM-CSIC.
[2] ETSIAAB-UPM.

https://doi.org/10.1016/j.compag.2022.106684
Received 23 July 2021; Received in revised form 15 November 2021; Accepted 1 January 2022
Available online 13 January 2022

(a) Robotic platform in a small cabbage row. The RGB camera is shown marked in red and the multi-spectral camera in yellow

(b) Robotic platform in a cabbage row: lateral view

Fig. 1. Robotic platform in cabbage rows. Source: Authors.

applied through irrigation systems distributed throughout the plantation (Asefpour Vakilian et al., 2017) or using high-capacity drones (del Cerro et al., 2021). This detection method has notable disadvantages due to light variations.

Notable works focused on plant detection and fertilization use very sophisticated platforms with a very high cost for spraying herbicide application on weeds (Lottes, 2021). There are also low-cost platforms, but their scope is very limited, as they only carry out monitoring tasks (Barusu et al., 2019). On the other hand, further developments have been made in crop monitoring to make decisions in fertilization processes (Arivalagan et al., 2020).

The SureVEG project investigates the benefits of diversified strip cropping systems for the intensive cultivation of organic vegetables, the development of automated machinery to manage them, and the reuse of biodegradable waste (CORE-Organic-Cofund, 2020). As part of this project a mobile robotic platform was developed, equipped with laser sensors, RGB and multi-spectral (MS) cameras, a spraying system and, a 5 degrees of freedom (DOF) robotic arm.

The objective for the algorithms in this work is to detect and characterize different vegetable species planted in single rows, i.e. to define the estimated radius and center position relative to the robot arm of cabbage and red cabbage plants. These parameters are then sent to the central core to execute the movement planning of the robot, and activate the fertilization system.

The detection and characterization (D.a.C.) is based on a robust algorithm based on an analysis performed by an artificial vision system and an implemented CNN that executes the process in real time. The entire proposed method is developed in ROS, which allows data management (sending and receiving) between the sub-systems of the robotic platform. The efficiency of the vegetables' D.a.C through the proposed method was validated by comparison with information previously acquired by the laser system, where the crop row was reconstructed from a preliminary pass of the platform and a first characterization of the plants was developed through point clouds (Krus et al., 2020). The decision-making on whether or not to fertilize a plant detected in the second pass of the platform is based on a multi-spectral (MS) analysis of NDVI parameters of the crop developed during the first pass (Cardim Ferreira Lima et al., 2020).

Furthermore, the employed vegetable detection method is compared to conventional methods that mainly use threshold techniques (Hemming and Rath, 2001; Tellaeche et al., 2011; Fue et al., 2020; Kurtulmus, 2014).

The main contributions of this article focus on implementing a robotic alternative for fertilization treatment at the single plant level based on individual vegetable detection and characterization using a robust algorithm that combines artificial vision and CNN. This work presents an integrated system capable of carrying out the entire process from data acquisition, processing through neural networks and decision making drive robotic actuators in real-time, using a low-cost platform. The application on a single plant level rather than larger areas, as well as the real-time detection and actuation set this work apart.

This paper is structured as follows: in Section 2, neural networks, the experimental fields, and the hardware and software are introduced in detail, followed by the results in Section 3. Finally, the conclusions in Section 4 summarize the main findings.

2. Materials and Methods

2.1. Robotic Platform and Field Test

The development of agricultural tasks requires equipment adapted to varying working conditions, such as uneven soil with small rocks, and less grip due to mud. A 4-wheel mobile platform (with approximate measurements of 1.6 $\times$ 1.5 $\times$ 0.8 $[m]$) was developed, using 45x45 aluminum profiles, allowing manual propulsion with $\leqslant 1[km/h]$ over the crop row. This platform is shown in the Fig. 1a-b. The components mounted on this platform are a robot with 5 degrees of freedom (DOF) from the Robolink Igus CPR, 3x Sick LMS-111 LiDARs, and two cameras: one nadir-looking Parrot Sequoia multi-spectral (MS) camera at a 1.5 $[m]$ height, and a Vorsch RGB camera at 1.4 $[m]$ at a 30 degree angle.

The field tests are performed at the ETSIAAB-UPM fields (40°26'33.1"N, 3°43'41.9"W), where two types of vegetables were planted: cabbage and red cabbage.

To perform the robotic fertilization process, two computers were used in a master–slave set-up. The master runs the neural network to identify the vegetables in real-time, with a 10th generation Intel i7 processor and an Nvidia Geforce GTX 1660Ti graphics card. It is connected to the slave through Wi-Fi using RosBridge. The slave controls the robot movement and the solenoid valve for fertilizer application, and has a 5th generation Intel i7 processor.

(a) RGB mosaic of a cabbage row.

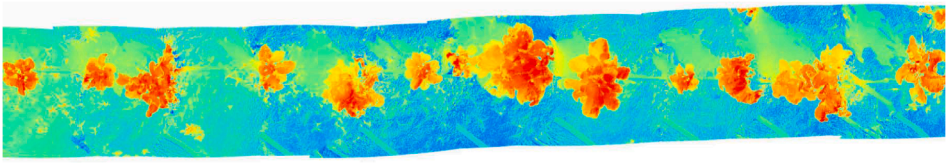

(b) Multi-spectral (NDVI) mosaic of the cabbage row.

(c) RGB mosaic of a red cabbage row.

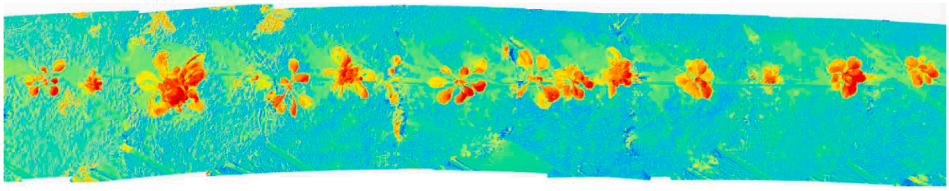

(d) Multi-spectral (NDVI) mosaic of the red cabbage row.

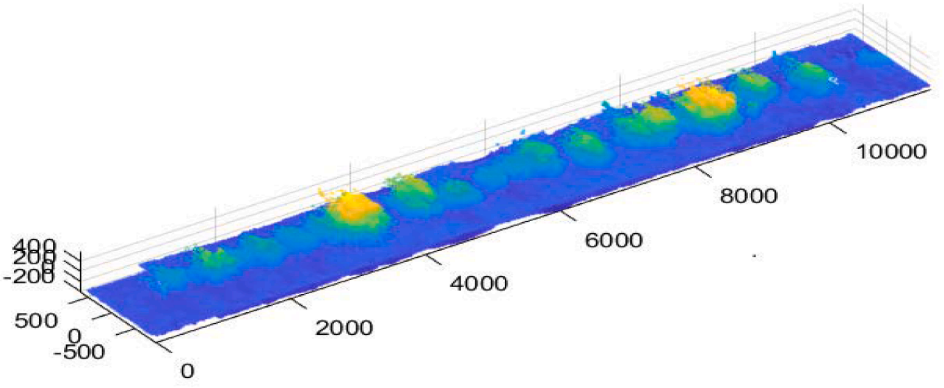

(e) Point cloud reconstruction of a cabbage row.

Fig. 2. RGB, multi-spectral (MS) and point cloud data acquired from crop rows. Source: Authors.

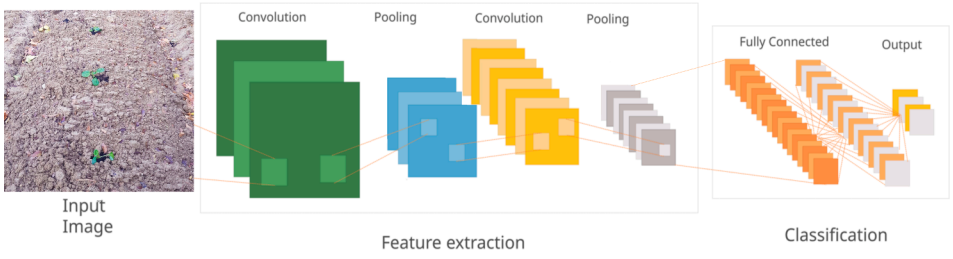

Fig. 3. Architecture of the CNN used. Source: Authors.

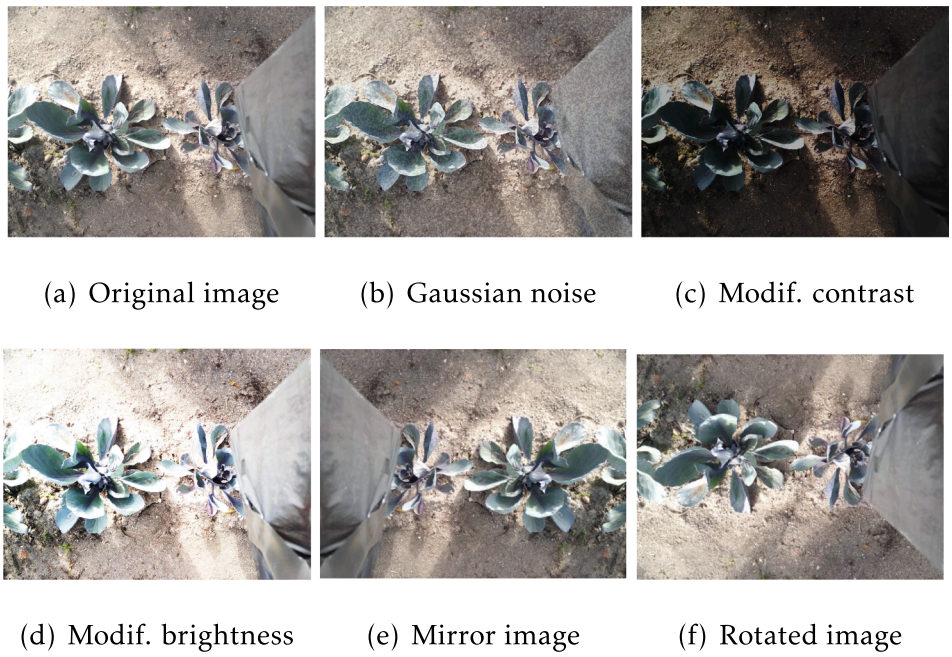

Fig. 4. Sample of the application of data augmentation to an image. Source: Authors.

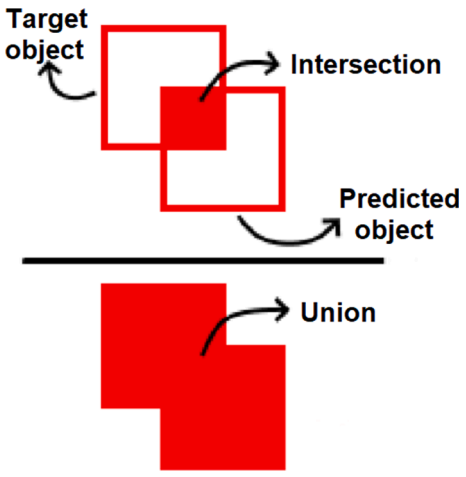

Fig. 5. Visualisation of the IoU metric. Source: Authors.

2.2. Data Acquisition from the Crop Rows

For the acquisition of the image data-set, the mobile platform was (manually) pushed over crop rows of 25 m long, at an approximate speed of 1 $[km/h]$. The multi-spectral sensor was programmed to acquire one set of images every 1.5 $[s]$, resulting in an overlapping area between images of 20%. The whole set of images was processed and stitched following the procedures developed in (Krus et al., 2021).

Figs. 2a-b each show a stitched RGB image of a cabbage and red cabbage row, from which the training data-sets are extracted. Figs. 2c-d show the corresponding NDVI values. These values were used to define which plants should or should not be fertilized using an NDVI analysis previously developed in (Cardim Ferreira Lima et al., 2020).

Fig. 2e shows the point cloud reconstructions of one of the rows. The location of the plants and estimated radius of the clusters are determined as described in (Cruz Ulloa et al., 2021) and were used to contrast the results obtained by the method proposed here.

The stitched mosaics were composed of the following number of images: cabbage (RGB: 45, MS: 180), red cabbage (RGB: 23, MS: 92), small cabbage (RGB: 28, MS: 112). The small cabbages are of the same variety as the other cabbages but in a different growth stadium.

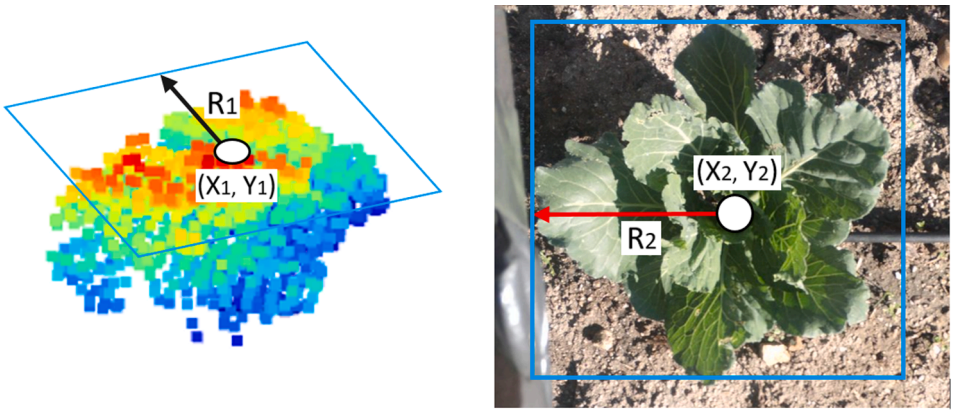

Fig. 6. Comparison of radius (R) and center (X, Y) of a plant in a point cloud $(_1)$ and a plant as detected through CNN $(_2)$. Source: Authors.

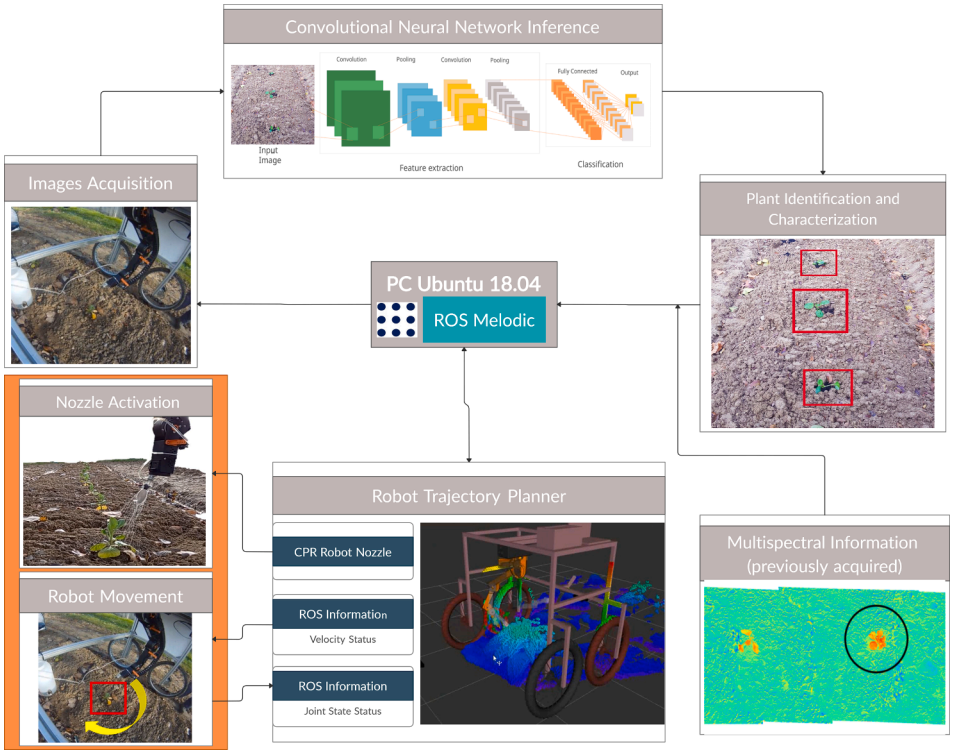

Fig. 7. Integration scheme of all the sub-systems to develop robotic fertilization using CNN. Source: Authors.

(a) Accuracy training for 100 epochs (each epoch has 630 batches).

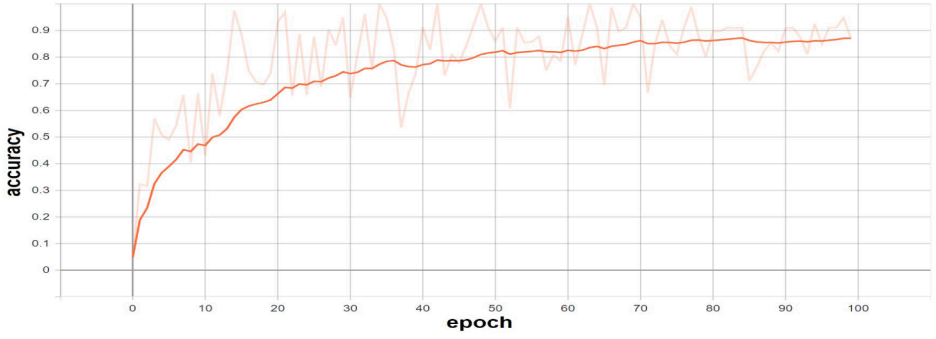

(b) Accuracy validation for 100 epochs.

Fig. 8. Accuracy training and validation curves. Source: Authors.

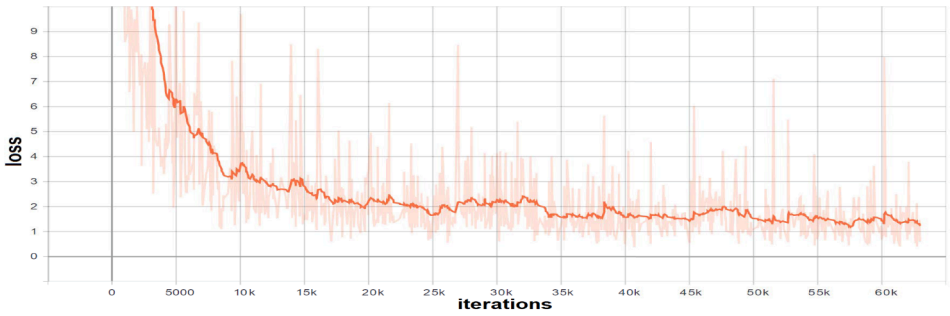

(a) Loss training for 100 epochs (each epoch has 630 batches).

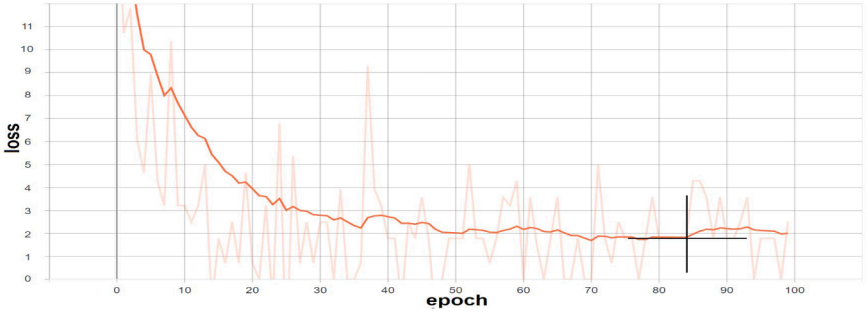

(b) Loss validation curve for 100 epochs. The black cross marks the validation curve's inflection point.

Fig. 9. Loss training and validation curves. Source: Authors.

2.3. Detection and Characterization Based on a CNN

The proposed algorithm is based on digital image processing. It takes one RGB image at a time (30 frames per second) by subscribing to a ROS topic from a camera mounted on the robotics platform, and applying operations to filter noise in the image. Subsequently, it runs the already trained neural network (inference process described below). The algorithm's outputs are: the plant (or plants) detected in an image, the bounding box with its center coordinates, and the estimated radius for each plant, which is calculated based on the bounding box.

2.3.1. CNN Architecture

The used network architecture is based on (Ikeda et al., 2018), as its main focus lies on recognizing objects. It has 24 convolutional layers and two fully connected layers. This network allows predicting the classes and coordinates within an image through its last layer (Duth and Jayasimha, 2020; Phung and Rhee, 2019).

Fig. 3 shows the CNN architecture, taking the images as input, followed by the features extraction phase through convolutions and pooling. Finally, in the classification phase the fully connected layers produce the recognized plant location(s) as a result, alongside their bounding box, and the recognition accuracy as a percentage.

The first phase of convolution finds characteristics of an image using detectors. These are different types of filters that group neighboring pixels to reduce the size of an image. In this way, several characteristic maps are obtained, which will move on to the next layer. A pooling layer reduces the size of the characteristic maps, where the ones that have the most influence on the final outcome are preserved, thereby aiding computational processing and avoiding potential over-training, while preserving detected features.

After 11 sets of convolution plus pooling, a flattening operation is applied, which converts the pooling result into a 1D vector per image. This vector serves as the input to the final fully connected layers, with internal weights established through back propagation.

For the network training, a technique known as transfer learning has been used, i.e. starting from a pre-trained network model for feature extraction. From that model, the last layers have been trained on our data-set. This makes the network capable of the classification of vegetables in the cultivation rows.

The algorithm has been developed in Python and can generate both the classification, detection of plants, and their location in the image. A bounding box marks the detected plants on the original image, based on the resulting descriptors: center location, length, and width.

Before image processing, the network applies a first re-scaling to 512 $\times$ 512 pixels and later to 256 $\times$ 256, 32 $\times$ 32, and 16 $\times$ 16. The network model initialization parameters were: batch (8), initial learning rate (0.001), decay (0.0005), and training steps (70000). The algorithms for convergence and error minimization were based on back propagation.

2.3.2. Training Data-Set

The training data-set has a set of 1638 images (each with a size of 1280x960), obtained in field tests at the initial growth phase and again after three months. An example of the crop rows is shown in Figs. 2a-b. The labels used to identify the data-set plants were: cabbage, red cabbage, small cabbage and small red cabbage, where a vegetable is considered 'small' if its diameter is less than 25 cm. The training was executed for 100 epochs to produce the vegetable detection model. Of the total image set, the ratio used for training and validation is: 70% (1146) and 30% (492), respectively.

Additionally, data augmentation was applied to the data-set's images because its application generates better results and improves robustness in the neural network to recognize objects (Dandavate and Patodkar, 2020; Pham et al., 2018). In that way, small alterations were applied through transformations applied to the data-set frames in Fig. 4. The employed techniques are mainly based on position augmentation (specifically scaling, rotation, translation, padding, and cropping), color

(a) Detected cabbages and small cabbages in the first half of Figure 2a.

(b) Detected cabbages and small cabbages in the second half of Figure 2a.

(c) Detected red cabbages and small red cabbages in the first half of Figure 2b.

(d) Detected red cabbages and small red cabbages in the second half of Figure 2b.

Fig. 10. Detection of crops in different rows. The recognized plant is marked with a red bounding box and a small label. Source: Authors.

augmentation (specifically brightness, contrast, and saturation), and noise reduction. This task was developed as a pre-training stage using a Python script that modifies and saves the new images.

The initially captured data-set was 1338 frames, of which 300 were altered using the aforementioned data-augmentation techniques. The originals of these altered images were also left in the data-set, resulting in 1638 images in total. The alterations ensured a wider range in light variations, contrast, and brightness in the training set to improve the system's robustness.

The result of the neural network is the plant class detected, its ac-

Table 1
Evaluation of the neural network's performance.

Crop ID	Precision	Recall	IoU
Cabbage	0.923%	0.916%	0.852%
Red Cabbage	0.905%	0.903%	0.837%
Small Cabbage	0.891%	0.912%	0.859%
Small Red Cabbage	0.867%	0.892%	0.862%

curacy percentage and coordinates (X, Y) relative to the fixed camera, with a position and orientation with respect to the robot base. This is obtained from the inference process of the trained network, and then combined with the original image through an overlay showing the bounding box, class name, and precision.

This data is used for two fundamental aspects of the fertilization work. The first one is defining the plant's position with respect to the robot, through rotation and translation matrices. Once this relative position is known, the semicircular path planning around the detected plant area with radius R can be generated, to apply the fertilizer through the nozzle placed at the robotic arm's end. The second one is optimizing the amount of fertilizer, based on the size of each individual plant.

The result of the training is a specific model with weights for each of the layers in the neural network. The final weights are used for the inference of new images in the validation set.

2.3.3. Metrics for Evaluation

The implemented detection efficiency algorithm takes the neural network evaluation results to define its efficiency in three terms: precision, recall, and intersection over union (IoU). Precision is defined as the ability of the model to identify only the relevant objects, recall is the ability to detect all objects present, and intersection over union (IoU) is defined as a metric to measure the object detector accuracy. Their equations are included in Eq. (1), following (Goutte and Gaussier, 2005), where *TP* denotes the number of true positives, i.e. the correct identification of a pixel belonging to a certain species. *FP* (false positives), on the other hand, denotes the number of pixels that were assigned to a species although those pixels did not actually show that species. Finally, false negatives are denoted by *FN* and describe the number of pixels that show vegetation but were wrongly identified as not containing a species. Fig. 5 illustrates the relationship between the predicted areas of a detected object and the object's original location to obtain the IoU parameter.

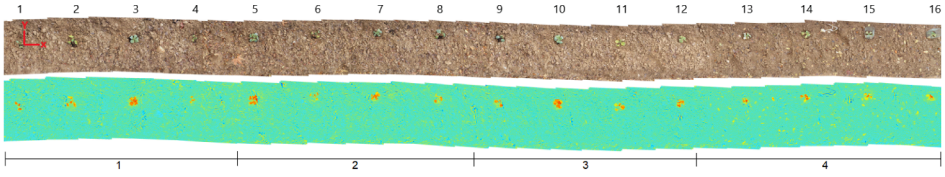

(a) RGB and NDVI mosaic of the crop row with 16 small cabbages, sectioned into 4 parts.

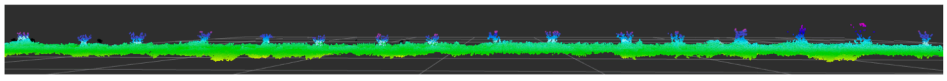

(b) Point cloud of the small cabbage row reconstruction, to validate data obtained from the neural network.

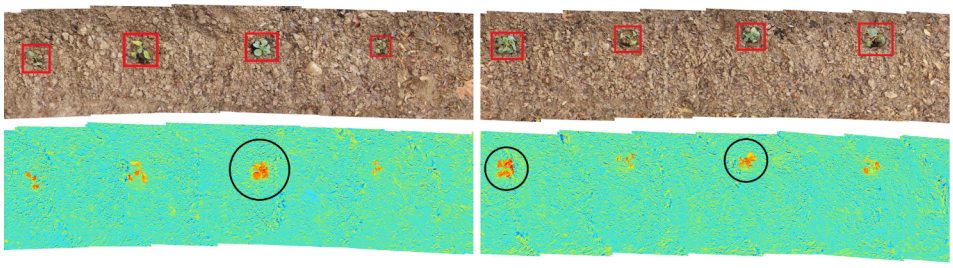

(c) 1st section. (d) 2nd section.

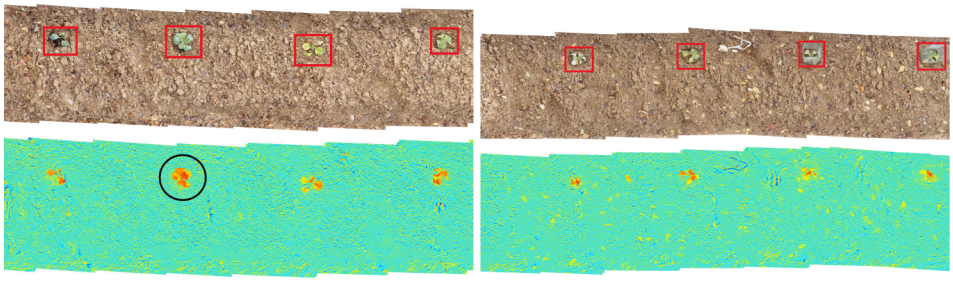

(e) 3rd section. (f) 4th section.

Fig. 11. Crop row with small cabbages for test execution. In (c), (d), (e), and (f) red boxes mark the detected plants through the neural network, and black circles indicate the plants that do not require additional fertilization. Source: Authors.

Table 2
Evaluation of the D.a.C. algorithm results for the small cabbage row in Fig. 11.

ID	Accuracy	$R[m]$	$X[m]$	$Y[m]$	e_R	e_X	e_Y
1	91.2%	0.0737	0.011	0.012	2.24%	1.21%	0.52%
2	90.3%	0.0783	0.513	-0.057	1.91%	2.6%	1.24%
3	92.5%	0.0728	1.022	−0.061	1.83%	3.4%	2.41%
4	88.3%	0.0625	1.485	−0.063	1.82%	3.0%	0.81%
5	91.7%	0.0732	2.039	−0.069	2.01%	3.8%	1.38%
6	88.4%	0.0691	2.522	−0.075	2.14%	2.4%	2.23%
7	89.9%	0.0710	3.033	−0.081	1.85%	3.6%	2.30%
8	91.1%	0.0743	3.512	−0.073	1.92%	2.4%	1.53%
9	90.7%	0.0686	4.014	−0.072	2.13%	2.8%	1.41%
10	91.6%	0.0692	4.506	−0.060	2.24%	3.2%	0.89%
11	92.3%	0.0703	5.032	−0.053	2.01%	3.4%	2.37%
12	88.2%	0.0692	5.523	−0.059	1.91%	3.9%	2.28%
13	87.8%	0.0684	6.042	−0.063	1.89%	3.4%	1.65%
14	90.3%	0.0767	6.531	−0.069	2.06%	3.2%	1.42%
15	89.4%	0.0782	7.012	−0.068	2.11%	2.4%	0.78%
16	89.6%	0.0751	7.513	−0.067	2.23%	2.6%	1.51%

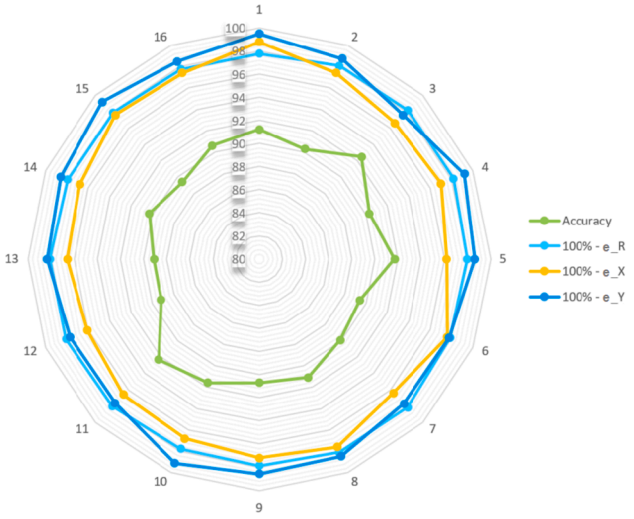

Fig. 12. Radial graph of the data in Table 2, the precision and complementary errors (100% - error) are shown for each plant in Fig. 11a. .Source: Authors.

$$\text{Precision} = \frac{TP}{TP + FP} \tag{1a}$$

$$\text{Recall} = \frac{TP}{TP + FN} \tag{1b}$$

$$\text{IoU} = \frac{\text{Intersection}}{\text{Union}} \tag{1c}$$

During the network training, the loss and accuracy curves are generated to evaluate their evolution and determine the best time to obtain the inference parameters (weights) of the neural network.

The radius (R) and central position (X, Y) results of the proposed algorithm are compared to previously acquired dimensions obtained through point clouds (radius and center of the clusters) in order to analyze the efficiency of the algorithm. Although the point cloud location and characterization process is quite adequate, it requires high computational processing and costly sensors. Fig. 6, shows the variables of the parameters to be evaluated and their arrangement in a 3D cluster and a 2D image. The percentage errors of the radius R, position X, and position Y, are analyzed as shown in Eq. (2).

$$e_R = \frac{|R_1 - R_2|}{R_1} \tag{2a}$$

$$e_X = \frac{|X_1 - X_2|}{X_1} \tag{2b}$$

$$e_Y = \frac{|Y_1 - Y_2|}{Y_1} \tag{2c}$$

2.4. Structure of the Automatic Robotic Fertilization Process

The algorithms and system integration are developed in ROS. Fig. 7 shows the structure of the integrated system. In the first instance, the images are acquired by an on-board platform camera (Images Acquisition), the CV_Bridge tool transmits them to ROS and processes them with OpenCV. After that, with the previously trained neural network, the crop type is detected along with its central coordinates. Once the plant is detected, the system relies on previously processed information from the NDVI indices of the multi-spectral images to decide whether or not it needs fertilization.

As described in Section 2.1, the camera's fixed position and the robot base's position on the implemented platform are known a priori. The camera is fixed to the platform and remains therefore fixed, regardless of the robotic arm's movements. The relative position of an object to the robot can be obtained using the known, and fixed, relations robot-world and world-camera. These positions are established using the eye-to-hand method for kinematic control.

For fertilization, the location and radius parameters are sent to the next stage (Robot Trajectory Planner) to calculate the path that the robotic arm must perform around the current plant to fertilize it (activating the nozzle during this process).

3. Results

3.1. CNN Training and Validation

The model's performance was analyzed based on the accuracy and validation training curves. In each epoch, the weights of the neural network are saved after validation. For the final model, the weights are selected from previous epochs based on the loss validation curve.

The training was carried out for 100 epochs, each with 630 batches with a batch size of 2 images, resulting in a total of 63000 iterations. The training accuracy result in Fig. 8a shows increasing values of over 80% from iteration 32 k onward, with a maximal accuracy of 90.5%, and the validation result in Fig. 8b shows a maximal accuracy of 89.5%.

Alternatively, the training and validation loss curves in Figs. 9a and 9b show decreasing values that dip below 2% from iteration 32 k onwards. Looking at the loss validation curve shown in Fig. 9b the values rise again after epoch 84. The curve's inflection point has been marked with a black cross as a reference.

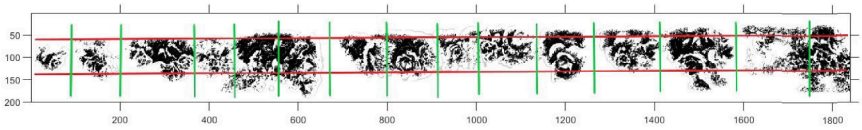

(a) Vegetable detection developed with conventional methods on the cabbage row shown in Figure 2a.

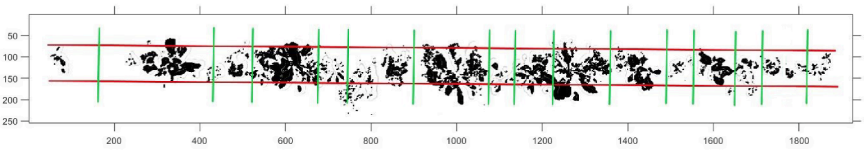

(b) Vegetable detection developed with conventional methods on the red cabbage row shown in Figure 2c.

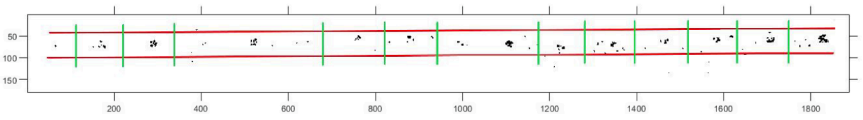

(c) Vegetable detection developed with conventional methods on the cabbage row shown in Figure 11a.

Fig. 13. Application of the conventional methods (such as (Tellaeche et al., 2011; Kurtulmus, 2014)) for detecting vegetables in rows, to the data collected in our fields. The rows are shown in red, and the sections in green correspond to the detected vegetables. .Source: Authors.

3.2. Vegetable Species Recognition in Row Crops

Fig. 10 shows the output of the trained neural network for (small) cabbage, and (small) red cabbage in different crop rows. The neural network's results are indicated by red boxes drawn on each recognized plant. Furthermore, a label is added to each plant.

The obtained result is satisfactory and verifies the training model before using it for robotic fertilization. The performance parameters of the network are shown in Table 1. Our model has a high precision value in all categories, the highest being the recognition of cabbage. While the lowest results were obtained for small red cabbage, the precision remains within the $[0.85 - 0.92]$ range, which indicates that the neural network does not have over-training and the results have a high level of confidence.

3.3. Evaluation of the Proposed Method

The implemented system's efficiency to detect and characterize the crops is validated with the metrics established in Section 2.3.3. These tests were carried out on a row of small cabbages shown in Fig. 11a with RGB and NDVI images, while Fig. 11b shows the reconstruction through point clouds, from which the reference values of the radii and centers were taken to establish the errors.

Figs. 11c-d-e-f each show parts of Fig. 11a. The detection (bounding boxes) are shown in red on the RGB images. In the NDVI image, the plants that require fertilization are indicated with a circle.

The fertilizing decision is based on the analysis of multi-spectral images, and the study of NDVI indices as developed in (Cardim Ferreira Lima et al., 2020; Krus et al., 2021).

Table 2 shows the results as calculated for this crop row (Fig. 11a), and Fig. 12 radially indicates the percentages of accuracy and errors (100% -error) for the calculated parameters. Based on these indicators, it can be concluded that the proposed method results have a high-reliability index with percentage errors below a mean of 3% and a mean accuracy of 90%.

3.4. Comparison of the Proposed Method to Conventional Detection Methods

Conventional methods are based on the detection of plants in crop rows; they are based on the uniform distribution of the crop and the use of classical vision techniques. However, the non-uniform growth of plants and environmental factors such as variable brightness, the influence of shadows, and the presence of weeds, limit the effectiveness of these methods.

The techniques of the conventional methods have been applied to our data to verify if there is a coincidence in the number of plants detected on the row. This comparison was performed on the cabbage row shown in Fig. 2a, the red cabbage in Fig. 2b, and the small cabbage in Fig. 11a). Fig. 13 shows the detected plants in each of these rows, where 15, 16, and 13 plants were detected out of the 13, 17, and 16 plants respectively. Our method, however, detects all of these plants reliably, despite variations in brightness and shadows or the presence of weeds.. This parameter has been precisely detected with our method.

Based on the amount of correct detection and the reduction in false matches for all three rows, efficiency values of 90.5% and 50.6% were obtained through the proposed method and the conventional methods, respectively.

Conventional methods do not have good applicability or satisfactory results when small vegetables and large vegetables are present in the same row, as these methods are based on thresholds, combined with erosion and image dilation techniques, to perform image segmentation and plant detection.

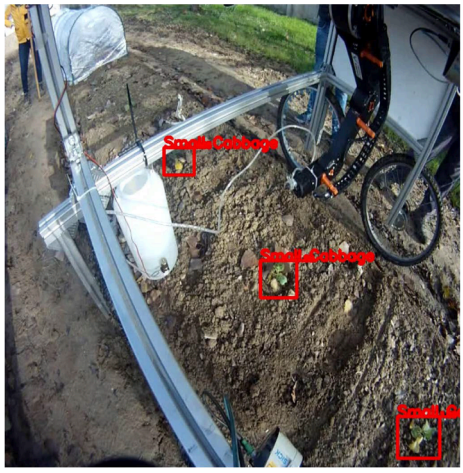

(a) Detection of three small cabbages using the RGB camera.

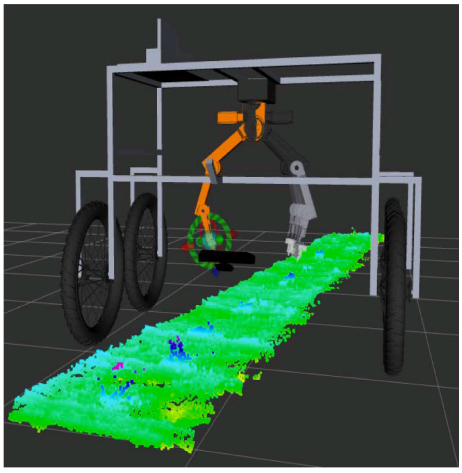

(b) Visualization of the robot's proprioceptive system in home position, using RVIZ.

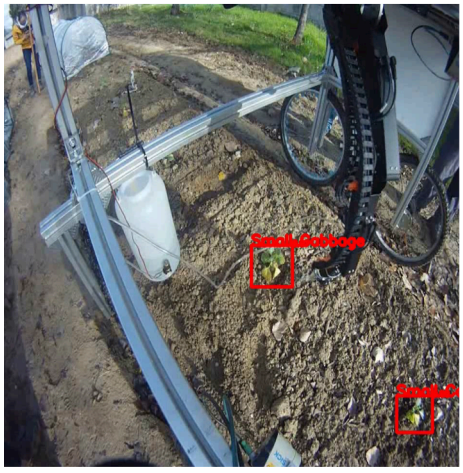

(c) Treatment application with the robot arm to the central small cabbage.

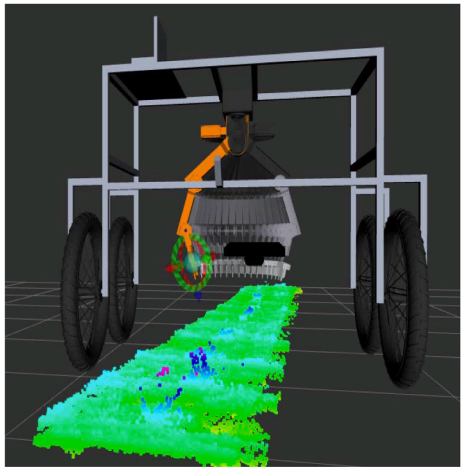

(d) Visualization of the robot's proprioceptive system during treatment application.

Fig. 14. Real time execution of vegetable detection and fertilization application in the crop row. Source: Authors.

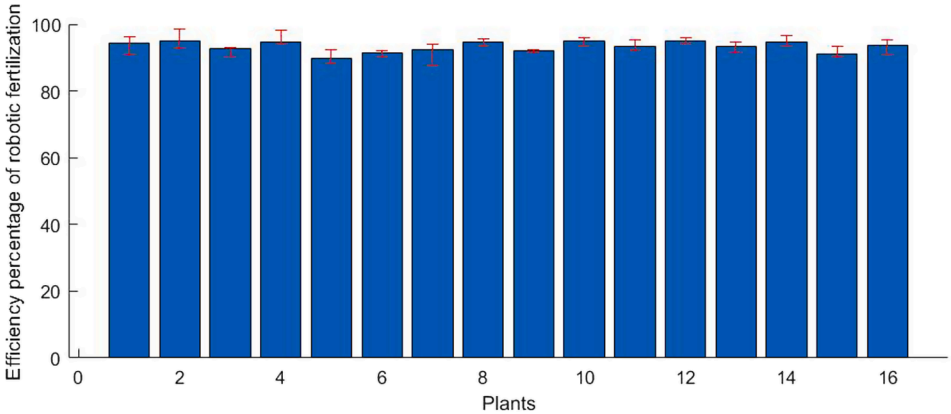

Fig. 15. Efficiency of robotic fertilization, in a (small) cabbage row (Fig. 11a), an average efficiency of 93% was obtained, depending on the analyzed parameters (trajectory execution, execution time, robotic arm's reach). .Source: Authors.

3.5. Fertilizer Application with the Robotic Arm

The robotic arm is attached to the platform, as shown in Figs. 14a-c. Fig. 14a shows the robot in the home position, with three small cabbages.

The decision of which plants should be treated first, is based on the closest plant to the center axis of the robot base. This is evaluated by the rotation and transformation matrices of the current position of the camera concerning the robot base.

Based on the crop parameters determined by the implemented algorithm (relative positions and treatment necessity), the movement planning algorithm determines the optimal path that the nozzle at the end of the robotic arm should perform to apply the fertilizer at the plant's base. Robot movements are executed through a series of positions and speeds as given by the planner.

Fig. 14c shows the robot applying the liquid treatment based on the plant's radius R. The sensory system of the position of the robot's state and the crop row reconstructed with point clouds is shown in Fig. 14b with the robot in the home position; then it moves according to the path defined by the planner, as shown in Fig. 14d.

The fertilizer application is carried out by opening a solenoid valve controlled by the central core system. The solenoid valve actuation is activated when the robot's end arrives at the plant's base and turns off when the robot has circled the entire base.

The efficiency of robotic fertilization was verified based on the correct trajectory execution, the nozzle opening, the execution time, and the robotic arm's reach for each plant. The strategy established to cover the entire plant is based on a circle, performed by the robot's end, while avoiding collision of the arm with the vegetation at any height. This collision avoidance and prescribed circular base result in a cone shape around the detected plant.

To verify compliance with the trajectories and times executed by the robot, the ROS viewer, RVIZ (ROS Viewer) was used, which allows collecting the sensory data shown in Fig. 14b-d. The reconstruction point clouds of the row is included alongside the positions of the robot during operation. Fig. 15, shows the efficiency of fertilization along the row of cultivation with small cabbage (Fig. 11a).

The main results of the efficiency of robotic fertilization show an average efficiency of 93%.

The proposed method optimizes the amount of liquid fertilizer applied to each single plant, while avoiding the application to bare soil. The path minimization criterion was used to optimize the fertilizer application process due to the defined cone strategy around the plant, to reach all plant areas and reduce the robot's movement time.

Future work could be the implementation of a neural network that is capable of distinguishing between desired crops and weeds. This system could then include a double solenoid valve actuation system, that on the one hand contains the fertilizer, and on the other hand the herbicides. Depending on the identified plant (vegetable or weed) in real-time, the robot would be able to position itself over the plant and apply the necessary treatment.

Alternatively, embedded systems such as Jetson Nano or Xavier type control cards could be integrated into this system, as they are capable of processing neural networks in real-time with low energy consumption.

The use of ROS for real-time processing of systems applied to agriculture has clear benefits to generic integrated systems, as demonstrated in this work. Most of the state-of-the-art projects focus on individualized systems such as the recognition of fruits or whole rows of cultivation via conventional methods. The proposed method has shown excellent robustness in situations like light variations, presence of weeds, etc. This has been corroborated by comparing the data with techniques that use conventional computer vision methods.

4. Conclusions

The proposed method based on CNN allows the automatic detection of cabbage and red cabbage in different sizes. The crops' characteristics (radius and central position relative to the robotic platform) obtained from the implemented algorithm have allowed the robotic arm planning and trajectory execution to apply the liquid organic fertilizer.

The different components of the implemented method: a robotic arm, sensory system, and CNN allow taking action at the individual plant level, considering specific sizes to dose liquid organic fertilizer. Different tests have validated the use of a low-cost RGB sensor (<20 €) over other systems such as laser processing.

The use of CNN for vegetable detection generated an algorithm that stands out over conventional systems of classical vision because of its robustness against environmental disturbances, especially light changes. Furthermore, the detection-characterization speed has a mean of 0.92 $[s]$.

The trained neural network has a high accuracy for recognizing these vegetable species. The performed tests reveal an average efficiency of 90.5% for crop detection and real-time execution. The curves shown in Figs. 8a and 9a show that, within 100 epochs, the loss and accuracy curves will have mean values of 2% and 90%, respectively, resulting in errors of $<3\%$ during the validation of the system.

Founding

This research was developed within the project "PCI2018-093074 Robot para el cultivo en hileras y reciclaje de residuos para la producción intensiva de vegetables y eficiencia energética", financed by Ministerio de Ciencia, Innovación y Universidades y la Agencia Estatal de Investigación, within the Projects program I + D+i Programacion Conjunta Internacional 2018 PCI-2018 and for the project "Sureveg: Strip-cropping and recycling for biodiverse and resource-efficient intensive vegetable production", within the action ERA-net CORE Organic Cofund: http://projects.au.dk/coreorganiccofund/. Also to Rob◦City2030-DIH-CM, Madrid Robotics Digital Innovation Hub, S2018/NMT-4331, funded by "Programas de Actividades I + D en la Comunidad Madrid".

Declaration of Competing Interest

The authors declare that they have no known competing financial interests or personal relationships that could have appeared to influence the work reported in this paper.

Acknowledgements

Special appreciation is given for the contribution made by Juan José Ramírez Montoro and Pablo Guillén Colomer during the development of field tests.

References

Álvarez-Canchila, O.I., Arroyo-Pérez, D.E., Patiño-Saucedo, A., González, H.R., Pati no-Vanegas, A., 2020. Colombian fruit and vegetables recognition using convolutional neural networks and transfer learning. J. Phys: Conf. Ser. 1547, 012020. https://doi.org/10.1088/1742-6596/1547/1/012020.

Arivalagan, M., Lavanya, M., Manonmani, A., Sivasubramanian, S., Princye, P., 2020. Agricultural robot for automized fertilizing and vigilance for crops. In: 2020 IEEE International Conference on Advances and Developments in Electrical and Electronics Engineering (ICADEE), pp. 1–3. https://doi.org/10.1109/ICADEE51157.2020.9368908.

Asefpour Vakilian, K., Massah, J., 2017. A farmer-assistant robot for nitrogen fertilizing management of greenhouse crops. Comput. Electron. Agric., vol. 139, pp. 153–163. doi:https://doi.org/10.1016/j.compag.2017.05.012. URL https://www.sciencedirect.com/science/article/pii/S0168169916312534.

Barusu, M., Reddy, K., Shanmugapriya, R., Barusu, M.R., 2019. Irrigation, fertilizing and weed cutting in the row crops with iot controlled robot. Int. J. Mech. Prod. Eng. Res. Development (IJMPERD) 8 (3). https://www.researchgate.net/profile/Madhusudhana-Reddy-Barusu/publication/331594285_IRRIGATION_FERTILIZING_AND_WEED_CUTTING_IN_THE_ROW_CROPS_WITH_IOT_CONTROLLED_ROBOT/links/5c828dae92851c695063df24/IRRIGATION-FERTILIZING-AND-WEED-CUTTING-IN-THE-ROW-CROPS-WITH-IOT-CONTROLLED-ROBOT.pdf.

Campos, Y., Sossa, H., Pajares, G., 2016. Spatio-temporal analysis for obstacle detection in agricultural videos. Appl. Soft Comput. 45, 86–97.
Campos, Y., Sossa, H., Pajares, G., 2017. Comparative analysis of texture descriptors in maize fields with plants, soil and object discrimination. Precis. Agric. 18 (5), 717–735.
Cardim Ferreira Lima, M., Krus, A., Valero, C., Barrientos, A., del Cerro, J., Roldán-Gómez, J.J., 2020. Monitoring plant status and fertilization strategy through multispectral images, Sensors 20 (2). doi:10.3390/s20020435. https://www.mdpi.com/1424-8220/20/2/435.
Manasa, S.C.N., Sharma, V., N.K.A.A., 2019. Vegetable classification using you only look once algorithm. In: 2019 International Conference on Cutting-edge Technologies in Engineering (ICon-CuTE), 2019, pp. 101–107. doi:10.1109/ICon-CuTE47290.2019.8991457.
CORE-Organic-Cofund, Sureveg project, https://projects.au.dk/coreorganiccofund/core-organic-cofund-projects/sureveg/, accessed on 27 August (12.08. 2020).
Cruz Ulloa, C., Krus, A., Barrientos, A., Del Cerro, J., Valero, C., 2021. Robotic fertilisation using localisation systems based on point clouds in strip-cropping fields. Agronomy 11 (1). doi:10.3390/agronomy11010011. https://www.mdpi.com/2073-4395/11/1/11.
Dandavate, R., Patodkar, V., 2020. Cnn and data augmentation based fruit classification model. In: 2020 Fourth International Conference on I-SMAC (IoT in Social, Mobile, Analytics and Cloud) (I-SMAC), 2020, pp. 784–787. doi:10.1109/I-SMAC49090.2020.9243440.
del Cerro, J., Cruz Ulloa, C., Barrientos, A., de León Rivas, J., 2021. Unmanned aerial vehicles in agriculture: a survey. Agronomy 11 (2). doi:10.3390/agronomy11020203. https://www.mdpi.com/2073-4395/11/2/203.
Duth, S., Jayasimha, K., 2020. Intra class vegetable recognition system using deep learning. In: 2020 4th International Conference on Intelligent Computing and Control Systems (ICICCS). IEEE, pp. 602–606.
Fue, K., Porter, W., Barnes, E., Li, C., Rains, G., 2020. Evaluation of a stereo vision system for cotton row detection and boll location estimation in direct sunlight. Agronomy 10 (8). doi:10.3390/agronomy10081137. https://www.mdpi.com/2073-4395/10/8/1137.
Gonzalez-de Santos, P., Fernández, R., Sepúlveda, D., Navas, E., Emmi, L., Armada, M., 2020. Field robots for intelligent farms–inhering features from industry, Agronomy 10 (11). doi:10.3390/agronomy10111638. https://www.mdpi.com/2073-4395/10/11/1638.
Gouel, C., Guimbard, H., 2019. Nutrition transition and the structure of global food demand. Am. J. Agric. Econ. 101 (2), 383–403.
Goutte, C., Gaussier, E., 2005. A probabilistic interpretation of precision, recall and f-score, with implication for evaluation. In: Losada, D.E., Fernández-Luna, J.M. (Eds.), Advances in Information Retrieval. Springer, Berlin Heidelberg, Berlin, Heidelberg, pp. 345–359.
HamidiSepehr, A., Mirnezami, S.V., Ward, J., 2019. Comparison of object detection methods for crop damage assessment using deep learning. CoRR abs/1912.13199. arXiv:1912.13199. URL http://arxiv.org/abs/1912.13199.
Hemming, J., Rath, T., 2001. Pa–precision agriculture: Computer-vision-based weed identification under field conditions using controlled lighting. J. Agric. Eng. Res. 78 (3), 233–243. https://doi.org/10.1006/jaer.2000.0639 https://www.sciencedirect.com/science/article/pii/S0021863400906395.
Ikeda, M., Sakai, Y., Oda, T., Barolli, L., 2018. Performance evaluation of a vegetable recognition system using caffe and chainer. In: Barolli, L., Terzo, O. (Eds.), Complex, Intelligent, and Software Intensive Systems. Springer International Publishing, Cham, pp. 24–30.
Krus, A., van Apeldoorn, D., Valero, C., Ramirez, J.J., 2020. Acquiring plant features with optical sensing devices in an organic strip-cropping system. Agronomy 10 (2). doi:10.3390/agronomy10020197. https://www.mdpi.com/2073-4395/10/2/197.
Krus, A., Valero, C., Ramirez, J., Cruz, C., Barrientos, A., del Cerro, J., 2021. Distortion and mosaicking of close-up multi-spectral images. In: Precision agriculture'21, Wageningen Academic Publishers, 2021, pp. 33–46.
Kulkarni, A.A., Dhanush, P., Chetan, B.S., Gowda, C.S.T., Shrivastava, P.K., 2020. Applications of automation and robotics in agriculture industries a review. IOP Conf. Ser.: Mater. Sci. Eng. 748, 012002. https://doi.org/10.1088/1757-899x/748/1/012002.
Kurtulmus, F., Kavdir, Ismail, 2014. Detecting corn tassels using computer vision and support vector machines. Expert Syst. Appl. 41 (16), 7390–7397. https://doi.org/10.1016/j.eswa.2014.06.013 https://www.sciencedirect.com/science/article/pii/S0957417414003546.
Kuznetsova, A., Maleva, T., Soloviev, V., 2020. Using yolov3 algorithm with pre- and post-processing for apple detection in fruit-harvesting robot. Agronomy 10 (7). doi:10.3390/agronomy10071016. https://www.mdpi.com/2073-4395/10/7/1016.
Li, Z., Li, F., Zhu, L., Yue, J., 2020. Vegetable recognition and classification based on improved vgg deep learning network model. Int. J. Comput. Intell. Syst. 13, 559–564. https://doi.org/10.2991/ijcis.d.200425.001.
Liu, J., Wang, X., 2020. Tomato diseases and pests detection based on improved yolo v3 convolutional neural network. Front. Plant Sci. 11, 898.
Liu, J., Wang, X., 2020. Tomato diseases and pests detection based on improved yolo v3 convolutional neural network. Front. Plant Sci. 11, 898. https://doi.org/10.3389/fpls.2020.00898 https://www.frontiersin.org/article/10.3389/fpls.2020.00898.
Lottes, Philipp, 2021. Plant classification systems for agricultural robots, Ph.D. thesis, Rheinische Friedrich-Wilhelms-Universität Bonn (Mar. 2021). URL https://hdl.handle.net/20.500.11811/8981.
Ma, J., Du, K., Zhang, L., Zheng, F., Chu, J., Sun, Z., 2017. A segmentation method for greenhouse vegetable foliar disease spots images using color information and region growing. Comput. Electron. Agric. 142, 110–117. https://doi.org/10.1016/j.compag.2017.08.023 https://www.sciencedirect.com/science/article/pii/S0168169917304672.
Magalhães, S.A., Castro, L., Moreira, G., dos Santos, F.N., Cunha, M., Dias, J., Moreira, A.P., 2021. Evaluating the single-shot multibox detector and yolo deep learning models for the detection of tomatoes in a greenhouse. Sensors 21 (10). doi:10.3390/s21103569. https://www.mdpi.com/1424-8220/21/10/3569.
Naik, N.S., Shete, V.V., Danve, S.R., 2016. Precision agriculture robot for seeding function. In: 2016 International Conference on Inventive Computation Technologies (ICICT), Vol. 2, 2016, pp. 1–3. doi:10.1109/INVENTIVE.2016.7824880.
Nguyen, V., Vu, Q., Solenaya, O., Ronzhin, A., 2017. Analysis of main tasks of precision farming solved with the use of robotic means. In: MATEC Web of Conferences, Vol. 113, EDP Sciences, 2017, p. 02009.
Oliveira, L.F.P., Moreira, A.P., Silva, M.F., 2021. Advances in agriculture robotics: A state-of-the-art review and challenges ahead. Robotics 10 (2). doi:10.3390/robotics10020052. https://www.mdpi.com/2218-6581/10/2/52.
Paoletti, M., Haut, J., Plaza, J., Plaza, A., 2019. A comparative study of techniques for hyperspectral image classification. Revista Iberoamericana De Automatica E Informatica Industr 16 (2), 129–137.
Pham, T.-C., Luong, C.-M., Visani, M., Hoang, V.-D., 2018. Deep cnn and data augmentation for skin lesion classification. In: Nguyen, N.T., Hoang, D.H., Hong, T.-P., Pham, H., Trawiński, B. (Eds.), Intelligent Information and Database Systems. Springer International Publishing, Cham, pp. 573–582.
Phung, V.H., Rhee, E.J., 2019. A high-accuracy model average ensemble of convolutional neural networks for classification of cloud image patches on small datasets. Appl. Sci., 9 (21). doi:10.3390/app9214500. https://www.mdpi.com/2076-3417/9/21/4500.
Ren, G., Lin, T., Ying, Y., Chowdhary, G., Ting, K., 2020. Agricultural robotics research applicable to poultry production: A review. Comput. Electron. Agric. 169, 105216. https://doi.org/10.1016/j.compag.2020.105216 https://www.sciencedirect.com/science/article/pii/S0168169919310427.
Sakai, Y., Oda, T., Ikeda, M., Barolli, L., 2016. A vegetable category recognition system using deep neural network. In: 2016 10th International Conference on Innovative Mobile and Internet Services in Ubiquitous Computing (IMIS), pp. 189–192. https://doi.org/10.1109/IMIS.2016.84.
Silva, V., Yang, X., Fleskens, L., Ritsema, C., Geissen, V., 2020. Soil contamination by pesticide residues-what and how much should we expect to find in eu agricultural soils based on pesticide recommended uses?. In: EGU General Assembly Conference Abstracts, p. 16476.
Steinbrener, J., Posch, K., Leitner, R., 2019. Hyperspectral fruit and vegetable classification using convolutional neural networks. Comput. Electron. Agric. 162, 364–372. https://doi.org/10.1016/j.compag.2019.04.019 https://www.sciencedirect.com/science/article/pii/S0168169918315680.
Sun, K., Wang, X., Liu, S., Liu, C., 2021. Apple, peach, and pear flower detection using semantic segmentation network and shape constraint level set. Comput. Electron. Agric. 185, 106150. https://doi.org/10.1016/j.compag.2021.106150 https://www.sciencedirect.com/science/article/pii/S016816992100168X.
Tellaeche, A., Pajares, G., Burgos-Artizzu, X.P., Ribeiro, A., 2011. A computer vision approach for weeds identification through support vector machines. Appl. Soft Comput. 11 (1), 908–915. https://doi.org/10.1016/j.asoc.2010.01.011 https://www.sciencedirect.com/science/article/pii/S1568494610000165.
Zeng, G., 2017. Fruit and vegetables classification system using image saliency and convolutional neural network. In: 2017 IEEE 3rd Information Technology and Mechatronics Engineering Conference (ITOEC), pp. 613–617. https://doi.org/10.1109/ITOEC.2017.8122370.
Zhang, Q., Karkee, M., 2021. Agricultural and field robotics: an introduction. In: Fundamentals of Agricultural and Field Robotics, Springer, 2021, pp. 1–10.
Zhang, S., Huang, W., Zhang, C., 2019. Three-channel convolutional neural networks for vegetable leaf disease recognition. Cognit. Syst. Res., vol 53, pp. 31–41, advanced Intelligent Computing. doi: 10.1016/j.cogsys.2018.04.006. https://www.sciencedirect.com/science/article/pii/S1389041717303236.